Anti-Corrosion potential of the Ortho and Para-Substituted Schiff Bases of 2-Methoxybenzaldehyde on Fe (110) surface in acid medium: Synthesis, DFT and Molecular Dynamics Studies

Collins U. Ibeji (✉ ugochukwu.ibeji@unn.edu.ng)

University of Nigeria

Damilola C. Akintayo

University of KwaZulu-Natal

Henry O. Oluwasola

University of Nigeria

Eric O. Akintemi

University of KwaZulu-Natal

Anti-Corrosion potential of the Ortho and Para-Substituted Schiff Bases of 2-Methoxybenzaldehyde on Fe (110) surface in acid medium: Synthesis, DFT and Molecular Dynamics Studies

Collins U. Ibeji*[1,2], Damilola C. Akintayo[3]*, Henry O. Oluwasola[1], Eric O. Akintemi[3]

[1]Department of Pure and Industrial Chemistry, Faculty of Physical Sciences, University of Nigeria, Nsukka 410001, Enugu State, Nigeria.

[2]Catalysis and Peptide Research Unit, School of Health Sciences, University of KwaZulu-Natal, Westville Campus, Durban 4041, South Africa.

[3]School of Chemistry and Physics, University of KwaZulu-Natal, P.M.B. X54001, Durban, 4000, South Africa.

*Corresponding authors: ugochukwu.ibeji@unn.edu.ng (C. U. Ibeji). ORCID: 0000-0003-4762-2256; damilolaakintayo141@gmail.com (D. C. Akintayo). ORCID: 0000-0003-1742-3571

Abstract

Corrosion inhibition potential of two synthesised Schiff base ligands; (E)-2-((2-methoxybenzylidene)amino)phenol **L1** and (E)-2-((4-methoxybenzylidene)amino)phenol **L2** were carried out by Density Functional Theory (DFT) and Molecular dynamics (MD) methods and theoretically explain the inhibitors' intrinsic properties and adsorption mechanism in the corrosion study. The adsorption mechanism of inhibitor on the surface of the Fe metal occurred via chemisorption inferred from the Gibbs free energy (ΔG_{ads}). Scanning electron microscopy (SEM) showed a mild degradation on the surface of the mild steel immersed in the **L1,** and **L2** inhibited acid solution, which could be because of surface coverage. DFT calculations revealed that the hybrid B3LYP functional performed better than M06-2X meta-functional in determining the energies of the synthesized Schiff bases for corrosion inhibition giving lower ΔE values 3.86 eV and 3.81 eV for **L1** and **L2.** The MD simulation revealed that the orientation of inhibitors on the surface of the metal resulted in the coordination bond formation and that the interaction energy of **L2** was -746.84 kJ/mol compared to -743.74 kJ/mol of **L1.** The DFT and MD results were in agreement.

Keywords: synthesis Schiff base; Corrosion inhibition; MD simulation

Introduction

Iron-based materials and low-alloyed metals are useful in several industrial applications and, they play important roles due to their structural and mechanical strength[1-3]. Mild steel is a type of ferrous alloy that has been used extensively in various industrial applications such as in the fabrication of cooling systems, pipes and space vehicles[4,5]. These metals and alloys become corroded due to the application of mineral acids[6-8]. Corrosion inhibition of mild steel using organic compounds, including natural products[9,10], synthetic and some inorganic compounds[7,11] has attracted much interest in recent years. These compounds serve as corrosion inhibitors because of the presence of heteroatoms such as nitrogen, oxygen, sulphur and π-electrons that promote adsorption on the metal surfaces thereby minimizing the deterioration of metals and their alloys in acid medium [2]. Schiff bases have been reported to be excellent corrosion inhibitors of corrosion due to the presence of the imine group that coordinates with the metal ions[3]. The inhibition efficiency of any given Schiff base ligand depends primarily on the type of *P*-orbitals, orbitals of the metal ions and the acid medium[12,13]. The structural and electronic properties of the compound are also a determinant, therefore, to comprehend the mechanism of inhibition between the surface of the metal and the inhibitor, Monte Carlo Simulation and quantum mechanics calculations are expedient. Many accounts regarding Schiff bases as corrosion inhibitors have been reoprted, However, scanty work exits on the effect of ortho and para directing groups in compounds as corrosion inhibitors. Therefore, this work reports the synthesis of ortho and para-substituted (E)-2-(methoxybenzylidene)amino)phenol Schiff base ligands, Density Functional Theory (DFT) and Monte Carlo Simulation to understand the adsorptive capacity and mechanism inhibitor and metal ion interactions

Experimental methods

Materials and methods

2-aminophenol, 2-methoxybenzaldehyde and 4-methoxybenzaldehyde were also obtained from Sigma-Aldrich and used without further purification. ^{1}H- and ^{13}C-NMR spectra were measured at room temperature using a Bruker 400 MHz spectrometer, their data were recorded in CDCl$_3$, with a residual internal solvent signal of 7.26 and 77.00 ppm, respectively. FT-IR spectra reported in wavenumbers (cm^{-1}) were obtained on a Perkin Elmer FT-IR spectrometer equipped with universal ATR. Mass spectra of the compounds were obtained from a Water synapt GR electrospray positive spectrometer. The electronic

absorption spectra were obtained using UV-3600 Shimadzu UV-VIS-NIR spectrophotometer. Thermo Scientific FLASH 20 0 0 CHNS/O Analyzers was used for Elemental analyses.

## General Synthesis of the Schiff base ligands

The Schiff base ligands (E)-2-((2-methoxybenzylidene)amino)phenol **L1** and (E)-2-((4-methoxybenzylidene)amino)phenol **L2** were obtained in excellent yields (97 – 98 %) by solvent-free grinding using a mortar and pestle (Scheme 1) according to commonly described protocol in literature [14,15]. The resultant products were dried in *vacuo* to completely remove the water and characterized spectroscopically using IR, NMR and UV-Vis.

Synthesis of L1

2-Aminophenol (1 mmol, 0.109g) was ground with 2-methoxybenzaldehyde (1 mmol, 0.136g) for 10 – 12 mins to obtain (E)-2-((2-methoxybenzylidene)amino)phenol **L1** as a yellow solid. Yield (3.36 g, 97%), M.Pt.: 100 - 102 °C. ^{1}H-NMR (CDCl$_3$ 400 MHz) δ (ppm) 3.95 (s, 3H), 6.92 (t, J=7.66 Hz, 1H), 7.01 (dd, J=8.24, 12.37 Hz, 2H), 7.08 (t, J=7.56 Hz, 1H), 7.20 (t, J=7.84 Hz, 1H), 7.35 (d, J=7.92 Hz, 1H), 7.49 (t, J=7.82 Hz, 1H), 8.18 (d, J=7.72 Hz, 1H), 9.21 (s, 1H). ^{13}C-NMR (CDCl$_3$ 400 MHz) δ (ppm) 153.1, 133.0, 128.5, 127.4. 120.09, 120.0, 116.1, 114.8, 111.3, 55.6. FT-IR (KBr, cm^{-1}): 3329 ν (O-H), 2933 ν (sp^3 C –H), 1587 ν (CH = N). MS-TOF m/z (%): 284.06 [*M* + *H]*$^+$ (*). Anal. Calcd. for C$_{14}$H$_{13}$NO$_2$: C, 73.99; H 5.77; N 6.16%. Found; C, 73.80; H 5.59; N 6.06.

Synthesis of L2

2-Aminophenol (1 mmol, 0.109g) was mixed with 2-methoxybenzaldehyde (1 mmol, 0.136g) to obtain (E)-2-((4-methoxybenzylidene)amino)phenol **L2** as a yellow solid. Yield (3.36 g, 98%), M.pt.: 83 - 85 °C. ^{1}H-NMR (CDCl$_3$ 400 MHz) δ (ppm) 3.91 (s, 3H), 6.92 (t, J=7.64 Hz, 1H), 7.02 (d, J=8.68 Hz, 2H), 7.03 (d, J=6.28 Hz, 1H), 7.22 (t, 1H), 7.29 (d, 1H), 7.49 (t, J=7.82 Hz, 1H), 7.90 (d, J=8.71 Hz, 2H), 8.65 (s, 1H). ^{13}C-NMR (CDCl$_3$ 400 MHz) δ (ppm) 162.5, 156.6, 152.1, 135.9, 130.6, 128.9, 128.3, 120.1, 115.8, 114.8, 114.3, 55.5. FT-IR (KBr, cm^{-1}): 3338 ν (O-H), 2836 ν (sp^3 C –H), 1589 ν (CH = N). MS-TOF m/z (%): 284.06 [*M* + *H]*$^+$ (*). Anal. Calcd. for C$_{14}$H$_{13}$NO$_2$: C, 73.99; H 5.77; N 6.16%. Found; C, 73.85; H 5.55; N 6.10.
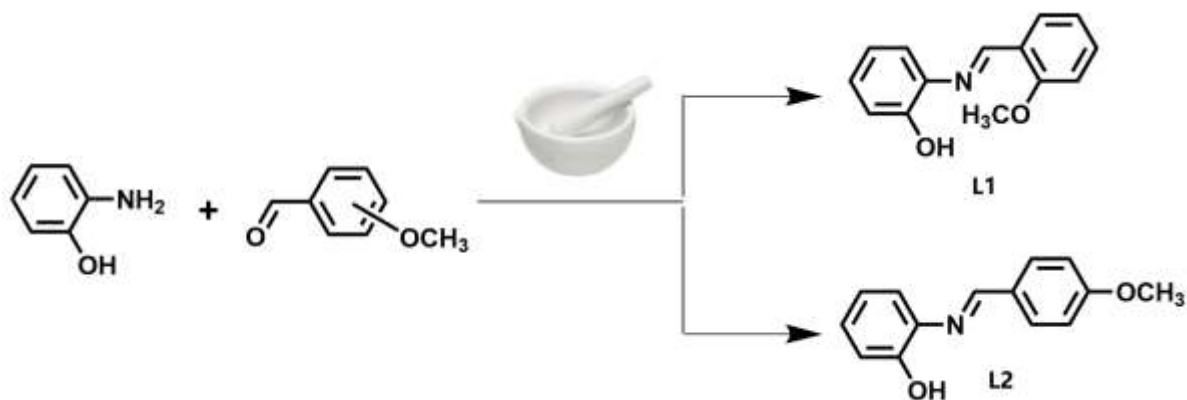
Scheme 1: Synthetic procedure for Schiff base ligands

Quantum mechanics calculations

The *ab initio* quantum mechanics calculations were performed to evaluate the molecule's chemical properties, including atomic charge and intra-molecular geometry [16]; stereo-electronic interactions accountable for conformational stability [17], and the selection of corrosion inhibitors [18] among others. In this study, the popular density functional theory (DFT)[19] method embedded in Gaussian 16 program [20,21] was used to investigate the electronic properties of newly synthesized Schiff bases for their reactivity and mechanism as a corrosion inhibitor. The hybrid density functional B3LYP [22] and the highly parameterized exchange-correlated M06-2X [23] functionals in combination with the 6-31+G(d,p) basis set [22] were chosen for the calculations and the results compared for their performances with respect to each variable. The Schiff bases **L1** and **L2** were modelled with GaussView 6 program and optimized to a minimum in gas-phase. The frequency calculations were performed on optimized geometries both in gas-phase and hydrochloric, HCl (ε=78.3, experimental solvent) media; and the results were compared for solvation effect. The fundamental conceptual DFT properties measured are the energies of the lowest unoccupied molecular orbital, E_{LUMO} and the highest occupied molecular orbital, E_{HOMO}. Other conceptual DFT parameters were determined from these basic properties in line with the work of Odewole *et al* [3] as expressed in equations (5) to (12).

$$\Delta E = E_{LUMO} - E_{HOMO} \qquad (5)$$

$$A = -E_{HOMO} \qquad (6)$$

$$I = -E_{LUMO} \qquad (7)$$

$$\eta = \frac{\Delta E}{2} \tag{8}$$

$$\delta = \frac{1}{\eta} \tag{9}$$

$$\chi = \frac{(I+A)}{2} \tag{10}$$

$$C_P = -\chi \tag{11}$$

$$\omega = \frac{\chi^2}{\Delta E} \tag{12}$$

Where ΔE is the energy gap, A is the electron affinity, I is the ionization potential, η is the chemical hardness, δ is the softness, χ is the absolute electronegativity, C_P is the chemical potential, ω is the global electrophilicity index.

The mechanism of inhibition was measured in terms of how electrons were transferred vis-à-vis the inhibitor and metal surface. In this case, the fraction of electron transferred, (ΔN) unto the metal surface was determined from the electronegativity and chemical hardness of both species as expressed in equation (13).

$$\Delta N = \frac{\chi_{Fe} - \chi_{inh}}{2(\eta_{Fe} - \eta_{inh})} \tag{13}$$

χ_{Fe} and χ_{inh} are the absolute electronegativity of iron and the inhibitor respectively while η_{Fe} and η_{inh} are the chemical hardness of iron and inhibitor respectively. The theoretical values 7 for χ_{Fe} and 0 for η_{Fe} were used according to a previous study by Ebenso and co-workers [24].

The local reactivity at various sites of the ligands was treated from the Mulliken atomic charges. These charges form the basic variables for deriving Fukui functions, namely nucleophilicity and electrophilicity, of the molecules according to equations (14) to (16) and were used to examine the the potential adsorption sites on the Schiff base molecules.

$$f_k^+ = [q_k(N + 1) - q_k(N)] \tag{14}$$

$$f_k^- = [q_k(N) - q_k(N - 1)] \tag{15}$$

$$\Delta f_k(r) = f_k^+ - f_k^- \tag{16}$$

Where f_k^+ and f_k^- are the nucleophilic and electrophilic Fukui functions, respectively. $q_k(N+1)$ and $q_k(N-1)$ are the charges on the atoms in a molecule in its anionic and cationic states, respectively. $q_k(N)$ is the charge on the atoms in a molecule in its neutral state.

Molecular dynamics simulation

Molecular dynamics (MD) simulation is known and has been applied to investigate the interaction of metal (Fe) surface and inhibitors. The MD simulation was carried out using Material Studio (Accelrys Inc)[25]. For better stability and the nature of the packed surface of the chosen metal surface, Fe (1 1 0) was used in this study. The relations between the inhibitor and the Fe (1 1 0) surface were performed in a simulation box size of 24.82 x 24.82 x 26.14 $Å^3$ thru periodic boundary conditions. A vacuum slab of 6 Å height was set up on the Fe (1 1 0). 200 molecules of water, 9 of Cl^- and 9 of H_3O^+[26] included using the Adsorption locator module in Material Studio. Geometric optimization was performed to obtain minimal structures. 5 cycles (2000 steps) of simulated annealing was applied and the MD was performed *via* Berendsen thermostat temperature control at 298 K and simulation time of 50 ps with 1 fs time step[27]. The simulation was carried out under canonical ensemble (NVT) and Condensed Phase Optimized Molecular Potentials for Atomistic Simulation Studies (COMPASS) force field[2,27,28]. The interaction energy was obtained, and the Radial Distribution Function (RDF) was computed. The interaction energies were obtained according to the equation (17)[27].

$$E_{interaction} = E_{total} - (E_{surface + H_2O + H_3O^+ + Cl^-} + E_{inhibitor}) \qquad (17)$$

E_{total} represents the total energy of the inhibitor molecule, surface, H_2O, H_3O and Cl^-, $E_{inhibitor}$ designates the energy of absorbed inhibitor on the surface and the $E_{surface}$ implies the energy of the metal surface involving H_2O, H_3O and Cl^-.

$$E_{binding} = -E_{interaction} \qquad (18)$$

Results and discussion

Spectroscopic Studies

The condensation of 2-aminophenol with the methoxybenzaldehydes produced the imine (C=N) functionality observed by a stretching band at 1587 and 1589 cm^{-1} on the IR spectra for **L1** and **L2** respectively (Figure S1 and S2). Additional bands observed around 3371,

2836, 1616 and 1250 cm^{-1} were assigned to ν(O—H), ν(C—H), ν(C=C) and ν(C—O), respectively [3]. Similarly, ^{1}H- and ^{13}C-NMR spectra of the ligands (Figure S3 – S6) afforded the imine proton and carbon peaks at 9.21 and 153.1 ppm for **L1** as well as 8.65 and 162.5 ppm for **L2** (Figure S5 and S6), which were further established the formation of the Schiff base [29]. The electronic absorption spectra of the ligands obtained in dichloromethane are shown in Figure 1. Due to intra-ligand charge transfer observed between 238 and 274 nm, absorption bands were assigned to $\pi \rightarrow \pi^*$ while the band around 350 nm was assigned to n $\rightarrow \pi^*$ transition [14].
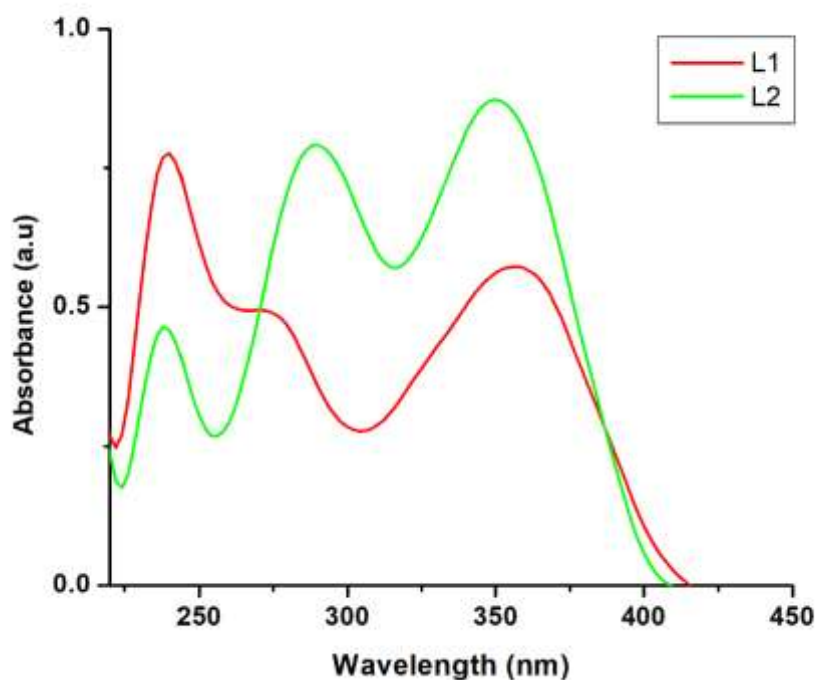
Figure 1: The electronic absorption spectra of the ligands obtained in dichloromethane

DFT analysis

Quantum electrochemical method through conceptual DFT analysis has demonstrated suitability in the field of corrosion science for either acid or base medium used for metal corrosion inhibition study [30]. A number of studies[26,31] have revealed the relationship between corrosion inhibition and the functional groups associated with the compounds under consideration. Analysis done with the b3lyp and m06-2x functional at 6-31+g(d,p) basis set are presented.

Optimized geometries and Energies analysis

Gaussian optimized structures of the Schiff bases are presented in Figure 2
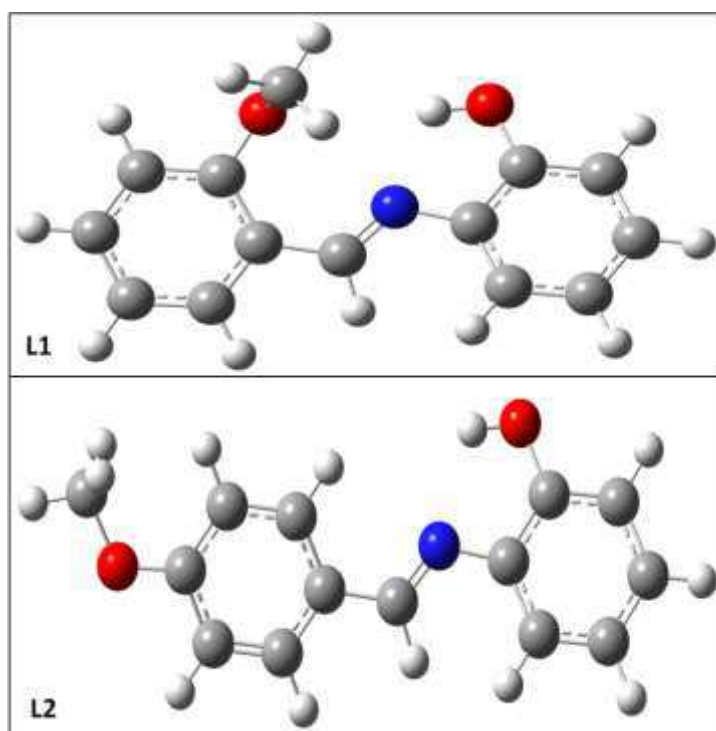
Figure 2: Optimized geometries of **L1** and **L2**

The work of Lgaz *et al* [31] supports the idea that inhibitor adsorption on the iron surface can proceed on a donor and acceptor reactions basis which link the unoccupied surface atom orbit and n electrons of the aromatic compounds. Table 1 shows energies of the LUMO and HOMO orbitals plus other conceptual DFT parameters. The higher HOMO energies obtained for both ligands in HCl solvent compared to gas-phase medium speed up the molecule's binding to the metallic surface and thus interferes with the electron transfer mechanism over the adsorbed layer. The energy gap, ΔE measures the minimum energy required for exciting an electron in the inhibitor molecule[32]. This study reveals that the hybrid B3LYP functional performs better than M06-2X meta-functional in measuring the energies of Schiff bases for corrosion inhibition because, the former gave much lower ΔE values of 3.86 eV and 3.81 eV for **L1** and **L2**, respectively as against 6.08 eV and 6.03 eV obtained with the later functional. Hence, the newly synthesized Schiff bases' inhibitory efficiency is better measured and higher with hybrid B3LYP functional.

Table 1: Electronic parameters and reactivity descriptors

	E_{LUMO} (eV)	E_{HOMO} (eV)	ΔE (eV)	A (eV)	I (eV)	η (eV)	δ (eV^{-1})	χ (eV)	C_p (eV)	ω (eV)	ΔN	μ (Debye)
L1, B3LYP (gas)	-2.16	-5.89	3.72	5.89	2.16	1.86	0.53	4.02	-4.02	4.35	0.79	3.49
L1, B3LYP (HCl)	-2.19	-6.06	3.86	6.06	2.19	1.93	0.51	4.12	-4.12	4.40	0.74	5.08
L1, M06-2X (gas)	-1.23	-7.17	5.94	7.17	1.23	2.97	0.33	4.20	-4.20	2.97	0.47	3.53
L1, M06-2X (HCl)	-1.28	-7.36	6.08	7.36	1.28	3.04	0.32	4.32	-4.32	3.07	0.43	5.00
L2, B3LYP (gas)	-1.99	-5.73	3.73	5.73	1.99	1.86	0.53	3.86	-3.86	3.99	0.83	3.57
L2, B3LYP (HCl)	-2.06	-5.88	3.81	5.88	2.06	1.90	0.52	3.97	-3.97	4.14	0.79	4.60
L2, M06-2X (gas)	-1.05	-7.02	5.96	7.02	1.05	2.98	0.33	4.03	-4.03	2.73	0.49	3.37
L2, M06-2X (HCl)	-1.14	-7.18	6.03	7.18	1.14	3.01	0.33	4.16	-4.16	2.87	0.46	4.16

Similarly, the chemical hardness is low in the hybrid B3LYP functional compared to M06-2X. This accounts for a relatively high softness and implies readily chemical reactivity as corrosion inhibitor. The $\Delta N > 0$ obtained for the ligand molecules reflects that they are very likely to donate electrons [33]. The viability and preference to use B3LYP functional over M06-2X for energies calculation is here confirmed since the former functional fraction of electron transferred as 0.74 and 0.79 (in HCl) for ligands **L1** and **L2** respectively as against 0.43 and 0.49 obtained using the later functional. The presence of aromatic rings and heteroatoms contribute to the corrosion inhibition efficacy of the molecules. By juxtaposing the two compounds using the energies analysis, **L2** is more effective as a corrosion inhibitor than the **L1** as demonstrated in the lower energy gap values and higher electron transferred fraction. In summary, the para-substituted ligand (**L2**) is relatively a stronger corrosion inhibitor of mild steel in HCl than its ortho-substituted (**L1**) derivative.

The frontier molecular orbital maps of the Schiff bases obtained with B3LYP/6-31+G(d,p) model in HCl solvent are presented in Figure 3. Maps from this model were chosen over the m06-2x model because the former gave a lower band gap which demonstrated a better measure of electronic properties of the Schiff bases. Ortho-methoxyl substitution in **L1** partly affects the electron distribution in the phenyl group joined to C9 making the C9 atom electron-deficient and it is the preferred site for electrophilic attack. This is demonstrated in

L1 where the electron cloud (HOMO-**L1**) spread from the C6 atom towards the phenyl group attached to it. In the same vein, electron cloud in **L2** spreads from the C6 atom towards the phenyl group attached to it, and electron cloud in phenyl group attached to C9 are evenly spread (HOMO-**L2**) and orbital maps facing each other. Thus, **L2** has a larger surface area with well spread electrons for transfer and to be adsorbed unto mild steel and this supports the previous suggestion that **L2** relatively enhanced inhibition of mild steel corrosion than **L1**. This is also buttressed in the fraction of electrons transferred since ΔN is higher in **L2** than in **L1**.
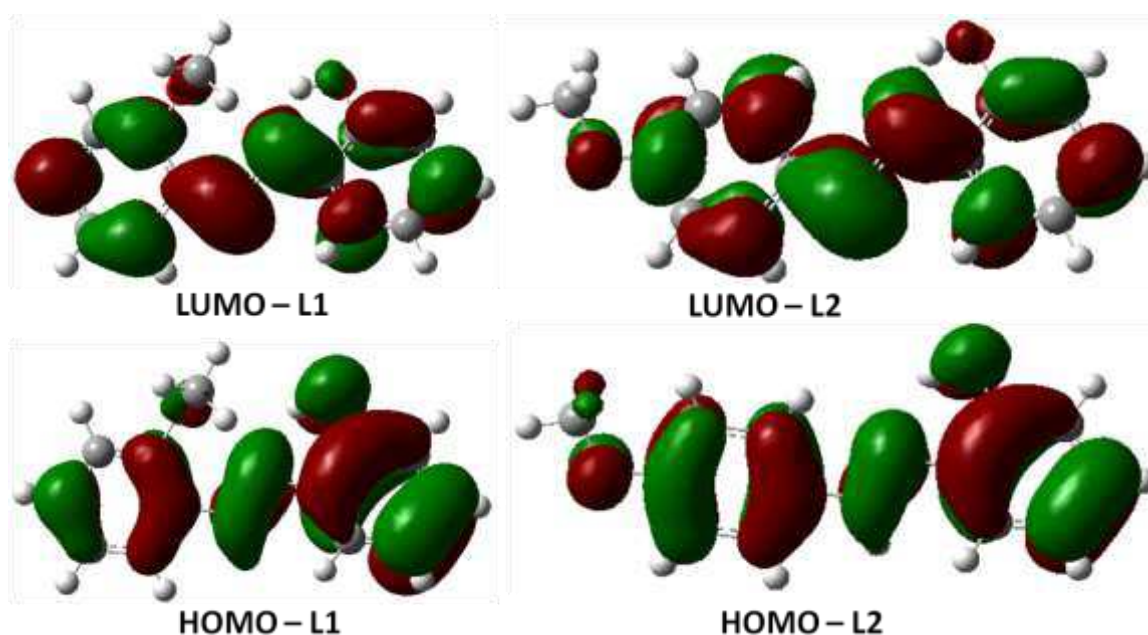
Figure 3: Frontier molecular orbitals of **L1** and **L2** calculated with B3LYP/6-31+G(d,p)

## Calculation of Fukui indices and Mulliken atomic charges

The Mulliken population analysis provides means of estimating partial atomic charges in evaluating the adsorption centres of inhibition and it is employed in determining the diffusion load across the whole inhibitor molecule system [26]. The Mulliken atomic charges and the respective Fukui function indices obtained are presented in appendices B3LYP /6-31+g(d,p) calculation for **L1** shows that C6 and C9 are the sites for nucleophilic and electrophilic attacks respectively in the gas-phase; while C15 and C10 are the sites for nucleophilic and electrophilic attacks respectively in HCl solvent. On the other hand, using M06-2X/6-31+G(d,p) for **L1** suggests that C6 and C9 are the respective sites for nucleophilic and electrophilic attacks in gas-phase and gas-phase HCl solvent.

Using B3LYP/6-31+G(d,p) for **L2** shows that C2 and C10 are the sites for nucleophilic attack both in gas-phase and in HCl solvent while C9 is the site for the electrophilic attack in both media. On the other hand, M06-2X/6-31+G(d,p) suggests that C2 and C10 are the sites for nucleophilic attack in gas-phase and HCl solvent respectively; while C11 and C9 are the sites for an electrophilic attack in gas-phase and HCl solvent. In summary, C6 and C9 are the respective preferred sites for a nucleophilic and electrophilic attack in **L1**; while C2 and C10 are the preferred sites for nucleophilic attack in gas-phase and HCl media while C9 is the preferred site for electrophilic attack in **L2**.

Molecular dynamics (MD) simulation

Molecular dynamics simulation has been reported to be a recognized method introduced to corrosion studies[34]. This approach gives insight into the inhibitors' interactions, orientation, and binding energies involving the inhibitors and metal surface[26,35]. In this work MD simulations were adopted to complement the experimental results obtained and to study the mechanism of interactions between the inhibitors and the Fe (1 1 0) surface as well as in the presence of 200 water, H_3O^+ and Cl^-. The surface configurations of the optimized inhibitors in the aqueous medium are presented in Figure 4. MD simulations showed that **L1** and **L2** inhibitors adsorb with a parallel configuration (Figure 4) firmly on the Fe (1 1 0) surface. This configuration resulted in the bond formation between the donor active site of **L1** and **L2** and the vacant orbitals of the positively charged Fe (1 1 0) surface[35]. The MD simulation revealed that notwithstanding the presence of the corrosive elements such as H_3O^+, Cl^- and the water molecules, a strong interaction exist between the surface of the metal and the

heteroatoms (O, N, and the phenyl ring) of **L1** and **L2**. The interaction energy of compounds unto the Fe (1 1 0) surface was calculated and **L1** gave a value of -743.74 kJ/mol, while **L2** had a value of -746.84 kJ/mol. The large positive value obtained mirrors the ability of the compounds to adsorb on the surface of the metal surface. The calculated interaction energy obtained is higher compared to that reported for other compounds[26,36]. The MD results indicated that the interaction energy for **L1** and **L2** agreed with the inhibition potential prediction obtained from DFT calcualtions. Based on the simulation, it can be inferred that the high interaction energy shows a slightly higher adsorption capabilities of **L2** on the surface of the metal which also suggests better adsorption stability with higher inhibition efficiency[37]. The length of the bond between Fe and heteroatoms was measured to determine the mechanism of adsorption. For L1, Fe-O (2.89 Å), Fe-N (3.21 Å) and Fe-C (2.87 Å), while for L2, Fe-O (3.09 Å), Fe-N (3.33 Å) and Fe-C (2.73 Å). Bond lengths between 1 and 3Å indicate chemisorption while >3.5 Å suggests physisorption mechanism[26]. Analysis showed that all the bond lengths of studied molecules with Fe surfaces are less than 3.5 Å indicating a chemisorption mechanism.

(a)

(b)
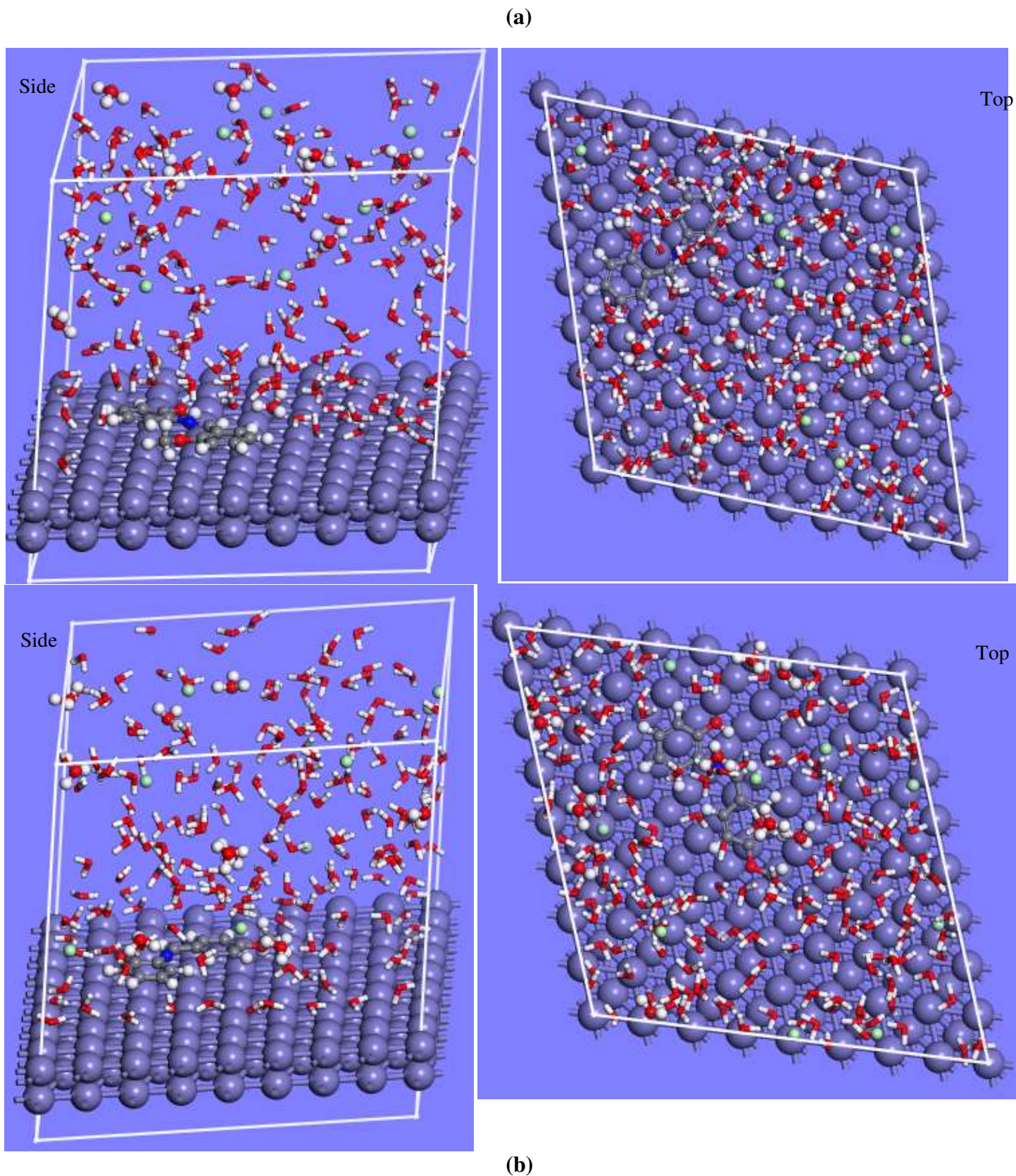
Figure 4. 3D depiction of the Side and top views showing suitable conformation for adsorption of (a) **L1** and (b) **L2** on Fe (110) surface in aqueous solution
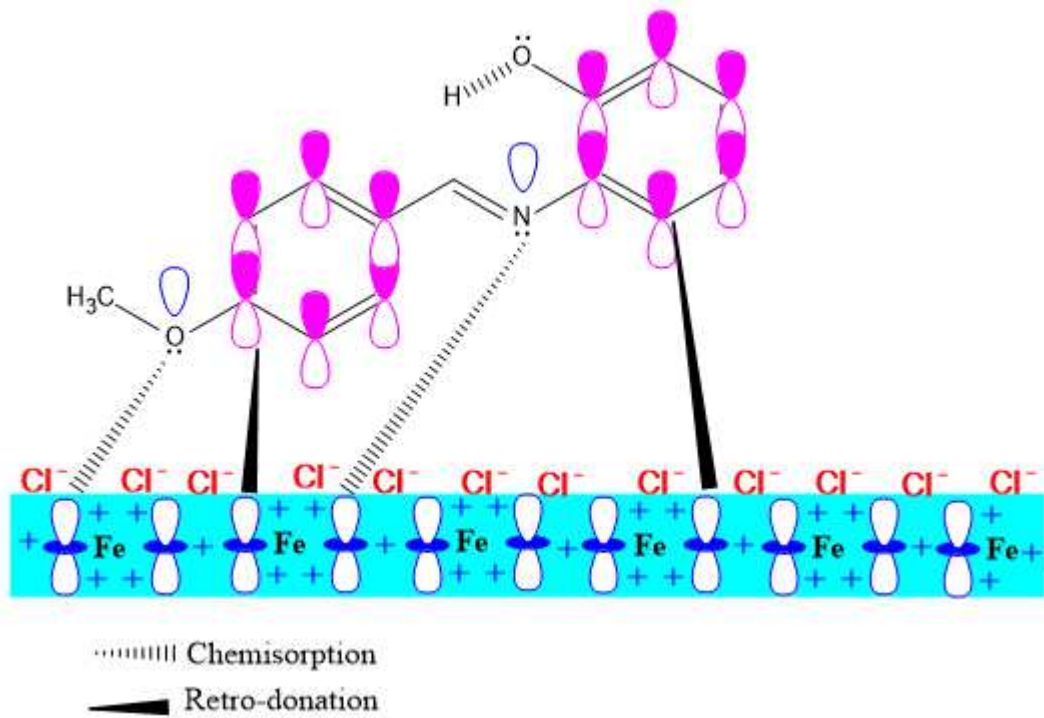
Inhibition mechanism

The corrosion inhibition mechanism of inhibitors depends largely on the adsorption of molecules on the metal surface which can be traced to factors such as the chemical structure of molecules under study[2,38]. The corrosion inhibition mechanism of compounds has been studied experimentally and *via* a theoretical approach. In this section, the mechanism of adsorption is discussed putting into consideration other components in the solution and the type of adsorption that occurs between Fe and **L1** and **L2. L1** and **L2** being Schiff base compounds could exist in the protonated form in 1.0 M Hydrochloric acid solution as seen in the following equilibrium:

$$L(y) + H^+ \leftrightarrow L(y)H^+ \tag{23}$$

Where y =1, 2

The resulting protonated form as shown in equation 23, shows that the adsorption of inhibitors on the metal surface promotes chemisorption. This is due to the electrostatic attraction that exist between the hydrated negative charges of Cl$^-$ on the surface of Fe (1 1 0) and the positive charges from the ligands[2,38]. Hydrogen gas is released as the protonated form of the Schiff base competes with the aqueous H$^+$, the heteroatoms of the ligands return to their neutral form, which then transfers unshared electron pair into the vacant orbitals of the Fe surface[2]. The series of transfers of electrons to the metal surface causes the accumulation of electrons in the metal. This results in a back the sequential transfer of electrons from the dd-orbitals of metal atoms to the unoccupied orbitals of the Schiff base leading to a phenomenon called chemisorption and retro-donation[35,39,40]. This results from the transfer of lone pair of electrons from the Schiff base formed and the pi electrons of the phenyl ring to the metal surfaces forming coordinate bonds. Figure 5 shows a pictorial explanation of the mechanism of corrosion inhibition.

Figure 5: Schematic representation of the adsorption mechanism of inhibitors on the Fe (1 1 0) surface in 0.1 M HCl

Conclusion

Schiff base ligands (E)-2-((2-methoxybenzylidene)amino)phenol and (E)-2-((4-methoxybenzylidene)amino)phenol were synthesized and characterized using NMR, IR and UV/Visible spectroscopy. The corrosion inhibition potential of these synthesized compounds was investigated using molecular dynamics approach and DFT approached. These methods were applied to elucidate their chemical reactivity and inherent properties. DFT calculations showed that the presence of aromatic rings and heteroatoms contribute to the corrosion inhibition efficacy of the synthesized compounds. The interaction energies obtained for L1 and L2 from molecular dynamics studies agree with the trend DFT.

Declaration of interest: Authors declare no conflict of interest.

Availability of data and materials: The data that support the findings of this study are available from Collins U. Ibeji, but restrictions apply to the availability of these data, which were used under license for the current study, and so are not publicly available. Data are however available from the authors upon reasonable request and with permission of Collins U. Ibeji

Authors Contribution

CUI designed and conceptualized, performed the molecular dynamics studies, and wrote part of the first draft. DCA, carried out the synthesis and wrote part of the draft of the paper. EOA performed the DFT studies and wrote a draft of the paper. HOO edited and revised the manuscript. All authors analyzed, read, edited, and approved the final manuscript.

Acknowledgements

References

1   Aouniti, A. *et al.* Schiff's base derived from 2-acetyl thiophene as corrosion inhibitor of steel in acidic medium. *Journal of Taibah University for Science* **10**, 774-785 (2016).

2   Okey, N. C. *et al.* Evaluation of some amino benzoic acid and 4-aminoantipyrine derived Schiff bases as corrosion inhibitors for mild steel in acidic medium: Synthesis, experimental and computational studies. *Journal of Molecular Liquids* **315**, 113773 (2020).

3   Odewole, O. A. *et al.* Synthesis and anti-corrosive potential of Schiff bases derived 4-nitrocinnamaldehyde for mild steel in HCl medium: Experimental and DFT studies. *Journal of Molecular Structure* **1223**, 129214 (2021).

4   Shivakumar, S. & Mohana, K. Corrosion behavior and adsorption thermodynamics of some Schiff bases on mild steel corrosion in industrial water medium. *International Journal of Corrosion* **2013** (2013).

5   Lgaz, H. *et al.* Experimental, theoretical and Monte Carlo simulation of quinoline derivative as effective corrosion inhibitor for mild steel in 1 M HCl. *J Mater Environ Sci* **7**, 4471-4488 (2016).

6   Abboud, Y. *et al.* 2, 3-Quinoxalinedione as a novel corrosion inhibitor for mild steel in 1 M HCl. *Materials chemistry and physics* **105**, 1-5 (2007).

7   Al-Amiery, A. A., Kadhum, A. A. H., Mohamad, A. B. & Junaedi, S. A novel hydrazinecarbothioamide as a potential corrosion inhibitor for mild steel in HCl. *Materials* **6**, 1420-1431 (2013).

8   Pandey, A., Singh, B., Verma, C. & Ebenso, E. E. Synthesis, characterization and corrosion inhibition potential of two novel Schiff bases on mild steel in acidic medium. *RSC advances* **7**, 47148-47163 (2017).

9   Oguzie, E. E. *et al.* Natural products for materials protection: Corrosion and microbial growth inhibition using Capsicum frutescens biomass extracts. *ACS Sustainable Chemistry & Engineering* **1**, 214-225 (2013).

10   Al-Haj-Ali, A. M., Jarrah, N. A., Mu'Azu, N. D. & Rihan, R. O. Thermodynamics and kinetics of inhibition of aluminum in hydrochloric acid by date palm leaf extract. *Journal of Applied Sciences and Environmental Management* **18**, 543-551 (2014).

11   Garcia-Ochoa, E. *et al.* Benzimidazole ligands in the corrosion inhibition for carbon steel in acid medium: DFT study of its interaction on Fe30 surface. *Journal of Molecular Structure* **1119**, 314-324 (2016).

12   Patel, A., Panchal, V., Mudaliar, G. & Shah, N. Impedance spectroscopic study of corrosion inhibition of Al-Pure by organic Schiff base in hydrochloric acid. *Journal of Saudi Chemical Society* **17**, 53-59 (2013).

13   Matar, S. A., Talib, W. H., Mustafa, M. S., Mubarak, M. S. & AlDamen, M. A. Synthesis, characterization, and antimicrobial activity of Schiff bases derived from benzaldehydes and 3, 3'-diaminodipropylamine. *Arabian Journal of Chemistry* **8**, 850-857 (2015).

14   Yusuf, T. L. *et al.* Design of New Schiff-Base Copper(II) Complexes: Synthesis, Crystal Structures, DFT Study, and Binding Potency toward Cytochrome P450 3A4. *ACS Omega* **6**, 13704-13718, doi:10.1021/acsomega.1c00906 (2021).

15   Adeleke, A. A., Zamisa, S. J. & Omondi, B. Crystal structure of dichlorido-bis ((E)-2-((pyridin-4-ylmethylene) amino) phenol) zinc (II), C24H20Cl2N4O2Zn. *Zeitschrift für Kristallographie-New Crystal Structures* **235**, 625-628 (2020).

16   Wu, H. S. & Sandler, S. I. Use of ab initio quantum mechanics calculations in group contribution methods. 1. Theory and the basis for group identifications. *Industrial & engineering chemistry research* **30**, 881-889 (1991).

17   Tormena, C. F. Conformational analysis of small molecules: NMR and quantum mechanics calculations. *Progress in nuclear magnetic resonance spectroscopy* **96**, 73-88 (2016).

18   Costa, J. & Lluch, J. The use of quantum mechanics calculations for the study of corrosion inhibitors. *Corrosion science* **24**, 929-933 (1984).

19   Argaman, N. & Makov, G. Density functional theory: An introduction. *American Journal of Physics* **68**, 69-79 (2000).

20   Robb, M. New Chemistry with Gaussian 16 & GaussView 6.

21   Frisch, M. *et al.* Gaussian 16, revision B. 01; Wallingford, CT, 2016. *Google Scholar There is no corresponding record for this reference*.

22   Tirado-Rives, J. & Jorgensen, W. L. Performance of B3LYP density functional methods for a large set of organic molecules. *Journal of chemical theory and computation* **4**, 297-306 (2008).

23   Walker, M., Harvey, A. J., Sen, A. & Dessent, C. E. Performance of M06, M06-2X, and M06-HF density functionals for conformationally flexible anionic clusters: M06 functionals perform better than B3LYP for a model system with dispersion and ionic hydrogen-bonding interactions. *The Journal of Physical Chemistry A* **117**, 12590-12600 (2013).

24   Ebenso, E. E., Isabirye, D. A. & Eddy, N. O. Adsorption and quantum chemical studies on the inhibition potentials of some thiosemicarbazides for the corrosion of mild steel in acidic medium. *International journal of molecular sciences* **11**, 2473-2498 (2010).

25   Inc, A. Materials studio release notes, Release 17.1. *Accelrys Software Inc., San Diego* (2017).

26   Chafiq, M. *et al.* Synthesis and corrosion inhibition evaluation of a new Schiff base hydrazone for mild steel corrosion in HCl medium: electrochemical, DFT, and molecular dynamics simulations studies. *Journal of Adhesion Science and Technology* **34**, 1283-1314 (2020).

27   Saha, S. K., Dutta, A., Ghosh, P., Sukul, D. & Banerjee, P. Adsorption and corrosion inhibition effect of Schiff base molecules on the mild steel surface in 1 M HCl medium: a combined experimental and theoretical approach. *Physical Chemistry Chemical Physics* **17**, 5679-5690 (2015).

28   Hsissou, R. *et al.* Evaluation of corrosion inhibition performance of phosphorus polymer for carbon steel in [1 M] HCl: Computational studies (DFT, MC and MD simulations). *Journal of Materials Research and Technology* **9**, 2691-2703 (2020).

29   Munzeiwa, W. A., Nyamori, V. O. & Omondi, B. N,O-Amino-phenolate Mg(II) and Zn(II) Schiff base complexes: Synthesis and application in ring-opening polymerization of ε-caprolactone and lactides. *Inorg. Chim. Acta.* **487**, 264-274, doi:10.1016/j.ica.2018.12.028 (2019).

30   Lashgari, M. & Malek, A. M. Fundamental studies of aluminum corrosion in acidic and basic environments: Theoretical predictions and experimental observations. *Electrochimica Acta* **55**, 5253-5257 (2010).

31   Lgaz, H. *et al.* On the understanding of the adsorption of Fenugreek gum on mild steel in an acidic medium: Insights from experimental and computational studies. *Applied Surface Science* **463**, 647-658 (2019).

32   Wazzan, N. A. DFT calculations of thiosemicarbazide, arylisothiocynates, and 1-aryl-2, 5-dithiohydrazodicarbonamides as corrosion inhibitors of copper in an aqueous chloride solution. *Journal of Industrial and Engineering Chemistry* **26**, 291-308 (2015).

33   Obot, I., Macdonald, D. & Gasem, Z. Density functional theory (DFT) as a powerful tool for designing new organic corrosion inhibitors. Part 1: an overview. *Corrosion Science* **99**, 1-30 (2015).

34   Lgaz, H., Salghi, R., Jodeh, S. & Hammouti, B. Effect of clozapine on inhibition of mild steel corrosion in 1.0 M HCl medium. *Journal of Molecular Liquids* **225**, 271-280 (2017).

35   Oukhrib, R. *et al.* DFT, Monte Carlo and molecular dynamics simulations for the prediction of corrosion inhibition efficiency of novel pyrazolylnucleosides on Cu (111) surface in acidic media. *Scientific reports* **11**, 1-18 (2021).

36   Singh, A. *et al.* Solvent-free microwave assisted synthesis and corrosion inhibition study of a series of hydrazones derived from thiophene derivatives: experimental, surface and theoretical study. *Journal of Molecular Liquids* **283**, 788-803 (2019).

37   Khaled, K. Molecular modeling and electrochemical investigations of the corrosion inhibition of nickel using some thiosemicarbazone derivatives. *Journal of Applied Electrochemistry* **41**, 423-433 (2011).

38   Gupta, N. K., Verma, C., Quraishi, M. & Mukherjee, A. Schiff's bases derived from l-lysine and aromatic aldehydes as green corrosion inhibitors for mild steel: experimental and theoretical studies. *Journal of Molecular Liquids* **215**, 47-57 (2016).

39   Daoud, D., Douadi, T., Issaadi, S. & Chafaa, S. Adsorption and corrosion inhibition of new synthesized thiophene Schiff base on mild steel X52 in HCl and H2SO4 solutions. *Corrosion science* **79**, 50-58 (2014).

40   Qiang, Y. *et al.* Synergistic effect of tartaric acid with 2, 6-diaminopyridine on the corrosion inhibition of mild steel in 0.5 M HCl. *Scientific reports* **6**, 1-14 (2016).

Supplementary Files

This is a list of supplementary files associated with this preprint. Click to download.

- Supportinginformation.docx